ORIGINAL ARTICLE

Identifying Sources of Atmospheric Pollutants in Densely Populated Urban Areas from a Particle Toxicity Perspective: a Study Using PMF Model and Vehicle Flux Analysis

Myoungki Song[1] · Seoyeong Choe[1] · Min Young Song[2] · Sung-Kyun Shin[2] · Sea-Ho Oh[1] · Hajeong Jeon[1] · Geun-Hye Yu[1] · Taehyoung Lee[3] · Min-Suk Bae[1]

Abstract

The aim of this study was to identify the sources of atmospheric pollutants in densely populated urban areas from a particle toxicity perspective. To this end, the Positive Matrix Factorization (PMF) model and vehicle flux analysis were used to identify the sources of atmospheric pollutants in an urban area based on the measured compounds and wind speed at the receptor site. Moreover, the toxicity of each emission source was compared with the dithiothreitol-oxidation potential normalized to 9,10-Phenanthrenequinone (QDTT-OP) analysis using the PMF source apportionment results. The study found that the dominant sources of atmospheric pollutants in the urban area examined were secondary product (43.7%), resuspended dust (25.4%), and vehicle emissions (14.4%). The vehicle flux analysis demonstrated that reducing the number of vehicles could directly reduce urban atmospheric pollutants. By comparing the time series of PMF source profiles with QDTT-OP, the QDTT-OP analysis showed an r^2 value of 0.9, thus indicating a strong correlation with biomass burning as the most harmful source of $PM_{2.5}$ based on emission sources. Overall, this study is expected to provide valuable guidance for managing atmospheric pollutants in densely populated urban areas, and the findings could serve as a helpful resource for improving urban air quality in the future.

Keywords QDTT-OP · Urban air pollutants · PMF · Biomass burning · Vehicle emission

1 Introduction

Air pollution is one of the top five risk factors for human health, with the other four being hypertension, smoking, obesity, and diabetes (Cohen et al. 2017; Forouzanfar et al. 2016). In the United States, air pollution is estimated to annually cause 130,000 deaths related to $PM_{2.5}$ and 4,700 deaths related to ozone, with an economic cost of $145 billion in health impacts as of 2005 (Fann et al. 2012; Im et al. 2018). The impact of air pollution is even more pronounced in developing countries with cities characterized by high-density urban areas such as Beijing, Jakarta, Bangkok, and Mexico City, where rapid urbanization is occurring (Yang et al. 2020). Unlike hypertension, smoking, obesity, and diabetes, air pollution is difficult to manage on an individual level, and it has a wide-ranging impact on urban areas. Therefore, national and global collaborative efforts are needed to minimize the adverse effects of air pollution on human health, and it is essential to identify the factors of air pollution that negatively affect human health.

Epidemiological studies have shown that particulate matter (PM) has a clear adverse impact on human health. For example, an increase of 10 μg/m³ of PM_{10} is associated with a 0.58% increase in mortality due to respiratory diseases, while an increase of the same concentration of $PM_{2.5}$ is associated with a 2.07% increase in the incidence of respiratory diseases (Dominici et al. 2006; Katsouyanni et al. 2001; Zanobetti et al. 2009). However, various studies have shown that the concentration of PM in the atmosphere does not have an absolute proportional relationship with its

✉ Min-Suk Bae
minsbae@mnu.ac.kr

[1] Department of Environmental Engineering, Mokpo National University, Muan, Republic of Korea

[2] Seoul Institute of Technology, Seoul, Republic of Korea

[3] Department of Environmental Science, Hankuk University of Foreign Studies, Yongin, Gyeonggido, Republic of Korea

harmful effects on human health; in fact, conflicting results have been reported (Bates et al. 2019). This may be due to the fact that the health effects of PM are influenced by its size and composition. For instance, particles smaller than 2.5 µm can penetrate the pulmonary alveoli and terminal bronchioles whereas particles ranging from 2.5 to 10 µm are mainly deposited in the primary bronchi. Meanwhile, particles larger than 100 µm are deposited in the nasal cavity, indicating that the effects of particles on the human body are determined by the organs that are affected by the particles, which is based on the particle size (Kelly and Fussell 2012). Moreover, PM's effects on human health can also be influenced by the presence of harmful substances in the particles. For example, the International Agency for Research on Cancer (IARC) classifies heavy metal components such as As, Cd, Cr(IV), and Ni are classified as group 1 carcinogens, while the IARC classifies polycyclic aromatic hydrocarbons (PAHs) in organic matter as class 1 or class 2 A carcinogens (IARC 2017; IARC 2010). Therefore, when the concentration of particles is similar, the adverse effects on human health are strongly influenced by the size of the particles and the substances they contain.

To evaluate the potential human health effects of PM in the atmosphere, it is necessary to analyze particle size and composition. However, determining the concentration, size, and composition of PM is a complex process that requires various analysis method, and it is not currently possible to identify all components of PM. As such, one method for assessing the potential harm of PM on human health is to measure the ability of PM to generate reactive oxygen species (ROS), which is defined as the oxidative potential (OP) (Delfino et al. 2011; Gao et al. 2020). This ROS-based approach differs from conventional methods that assess the harm of PM based on its characteristics, as it evaluates the potential harm of PM from the perspective of its production of ROS, which are known to cause human damage. One important mechanism by which PM causes human damage is by inducing a persistent state of inflammation, which is known to lead to various health risks, including epithelial cell inflammation, airway hyperresponsiveness, and lung damage, among others (Auerbach and Hernandez 2012; Berhane et al., 2011; Brown et al. 2012; Patel et al. 2013). Notably, when such inflammation is induced, ROS generated by PM are produced (Auerbach and Hernandez 2012; Esposito et al. 2014). Therefore, measuring the ROS induced by PM can be used to evaluate the potential harm of PM on human health, including its size, surface area, and chemical composition (Esposito et al. 2014; Gao et al. 2020; Lodovici and Bigagli 2011).

Urban areas with dense populations are highly affected by atmospheric pollutants, especially PM, which has a significant impact on human health. Moreover, as individual voluntary management is limited in its ability to mitigate the health effects of atmospheric pollutants, there is a need for governmental or intergovernmental efforts. The current efforts to reduce PM levels in urban areas have mainly focused on reducing the absolute amount of PM emissions. Policies aiming to reduce vehicle traffic and improve fuel quality, which targetsignificant contributors to PM emissions and generation in urban areas, are examples of such efforts (Matsumoto et al. 2006; Perrino et al. 2002). These policies can have a positive impact on reducing the health hazards of urban PM by reducing the absolute amount of PM. However, from a health hazard perspective, a reduction in the absolute amount of PM may not necessarily correspond to a proportional decrease in health hazards. Thus, existing efforts to reduce the absolute amount of PM may have lower cost-effectiveness in terms of reducing the health hazards caused by PM. To efficiently reduce the health hazards caused by atmospheric PM, it is necessary to identify the sources of PM with particularly high health hazards and manage them accordingly.

Therefore, the purpose of the current study is to analyze the characteristics of air pollutants in densely populated urban areas and identify the sources of air pollutants that pose a high risk to human health. To achieve this goal, urban air pollutants were observed and analyzed, and sources of air pollutants with a high risk to human health were identified based on the analysis results. This study also proposes a management plan for urban air pollutants based on vehicle flow, which is recognized as a major source of air pollutants in urban areas. The findings of this study are expected to serve as valuable data for managing air pollution in densely populated urban areas.

2 Model Description

2.1 Sampling Location and Period

As shown in Fig. 1, the monitoring station was installed in Gwanghwamun Square, between the statues of King Sejong and Admiral Yi Sun-sin. Gwanghwamun Square is a central square located in Seoul, South Korea that was newly expanded and redeveloped in 2022. The monitoring station was operated at a distance of approximately 3 m from the road. Sample collection for the observation and analysis of air pollutants was conducted from September 5th, 2022, 6:00 PM, to September 24th, 2022, 6:00 AM.

2.2 Real-Time Measurements

The real-time observations collected in the study area were meteorological parameters such as wind direction, wind speed, temperature, and humidity, as well as gas-phase compounds. The traffic flow around the measurement station
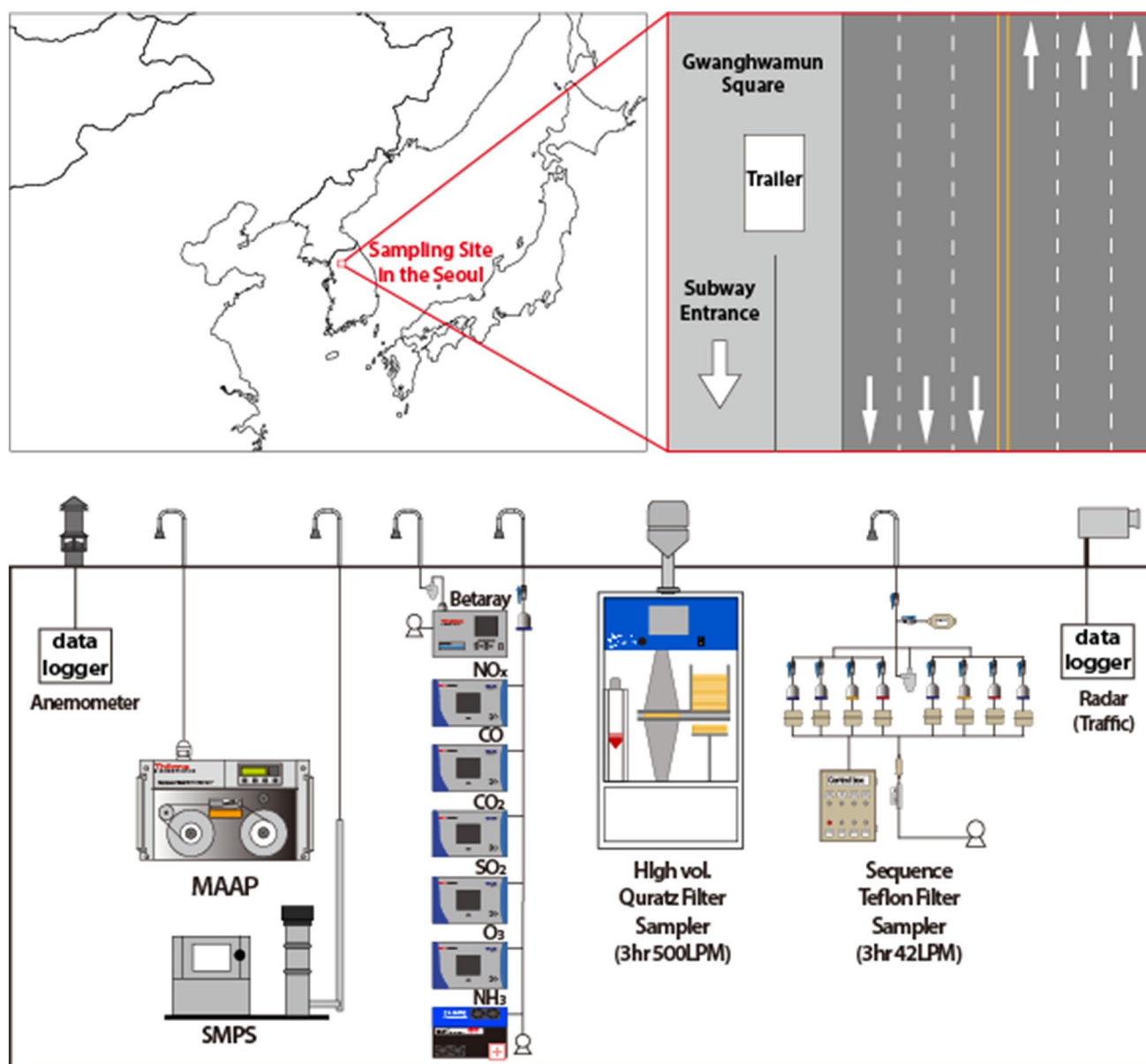
Fig. 1 Sampling location within the Seoul urban area and schematic diagram of air monitoring mobile station

was also observed using the HD Digital Wave Radar (Smart Sensor HD Model 126, Wavetronix, Provo, UT, USA). The meteorological parameters were measured using the static weather sensor EOLOS-IND (LAMBRECHT meteo, Germany), which is a real-time measuring instrument. The gas-phase substances were measured using real-time measuring instruments such as CO (infrared spectroscopy), CO_2 (infrared spectroscopy), SO_2 (ultraviolet fluorescence), O_3 (ultraviolet absorption), NO, NO_2 (chemiluminescence, Thermo Scientific, Waltham, MA, USA), and NH_3 (Los Gatos Research (LGR), ABB Inc., San Jose, CA, USA). The gas-phase measuring equipment was calibrated before measurement at a single point; after calibration, it was confirmed

that it measured within 5% of the target concentration by injecting different concentrations outside of the calibration range. The $PM_{2.5}$ concentration was measured in real-time using a beta-ray monitor (5014i Continuous Particulate Monitor, Thermo Scientific, USA). For quality control purposes, the $PM_{2.5}$ was collected on filters every three hours, after which the concentration was calculated based on the weight method, followed by beta-ray and equivalence evaluation. Equivalent Black Carbon (eBC) was measured using a Multi-angle Absorption Photometer (MAAP, Thermo Scientific 5012). The MAAP employs a technique of correcting for transmitted light by measuring the intensity of scattered light using photodetectors installed at the front and back of

the filter, thereby resolving issues arising from individual scattering phenomena of the filter-based equipment and the captured aerosols as well as their interaction. The particle number concentration by size was observed using the Scanning Mobility Particle Sizer (SMPS) (TSI Electrostatic Classifier Model 3082, Water-Based Condensation Particle Counter 3789, USA). The resolution of each observation item was one minute for meteorological and gas-phase compounds, one hour for $PM_{2.5}$, and ten minutes for particle number concentration. However, based on the resolution of $PM_{2.5}$ collection, all real-time observation items used three-hour average data.

2.3 Chemical Analysis of Semi-Real Time Samples

$PM_{2.5}$ was collected at 3-hour intervals (150 ± 10 samples) during the study period using a High-Volume Aerosol Sampler (DHA-80, Digitel Elektronik AG, Swiss). The collected $PM_{2.5}$ was analyzed for carbon components including OC, EC, and water soluble organic carbon (WSOC), soluble ion components including NO_3^-, SO_4^{2-}, and NH_4^+, elemental components including Al, Si, As, and Pb, organic molecular markers including levoglucosan, 1,2-benzene carboxylic acid (1,2-BCA), 1,4-benzene carboxylic acid (1,4-BCA), and methyl sulfonic acid (MSA), and oxidative potential for health risk assessments using Quinone dithiothreitol-oxidative potential (QDTT-OP) analysis. Carbon components including organic carbon (OC) and elemental carbon (EC) were analyzed using a Lab-based OCEC Carbon Aerosol Analyzer (Sunset laboratory Inc., USA) based on the protocol outlined by the National Institute of Occupational Safety & Health (NIOSH 5040). Soluble ions were quantified using an anion (Metrohm 930 Switzerland, Metrosp A Supp 150/4.0 column, 3.7 mM Na_2CO_3 & 1.0 mM $NaHCO_3$) and cation (Metrohm 930 Switzerland, Metrosep C4-250/4.0 column, 5 mM HNO_3) chromatography system after extraction with 10 mL distilled water from the cut filters utilizing a constant-temperature circulating water bath (CA-111, Eyela, Japan) connected to an ultrasonic bath (8800, Branson, USA) for 2 h. Elemental components were analyzed without special pretreatment using X-ray fluorescence spectrometry (XRF, Quant'X, Thermo Scientific, USA). Organic tracer components were extracted from cut filters with a 1:1 mixture of water and methanol, then analyzed using LC-QTof (LC: Agilent infinity ii, QToF: SCIEX X500r) with an SB-C18 column (Agilent Poroshell 120). Detailed information on the analytical methods used along with quality assurance/quality control (QA/QC) can be found in the previous studies referenced.

For the purpose of hazard assessment, analysis of dithiothreitol-oxidation potential normalized to 9,10-Phenanthrenequinone (QDTT-OP) was performed. QDTT-OP analysis is an improved method of DTT-OP (dithiothreitol-oxidative potential) analysis, which normalizes the decrease in DTT using 9,10-Phenanthrenequinone, and which is a method that enhances the original DTT-OP experiment (Choe et al. 2022). Briefly, the redox reaction DTT-OP experiment is performed by reacting the chemical components of $PM_{2.5}$ with dithiothreitol (DTT), and the residual DTT after reduction over time is observed in the form of 2-nitro-5-thiobenzoic acid (TNB) (Li et al. 2009). Therefore, it utilizes the DTT reduction rate caused by various chemical components, including reactive oxygen species (ROS) in $PM_{2.5}$ (Gao et al. 2020). However, the DTT reduction rate of the DTT-OP experiment depends on the initial concentration of DTT used in the analysis (Lin and Yu 2019). This makes it difficult to quantify human health hazards using DTT-OP. QDTT-OP is a method that improves upon the shortcomings of the original DTT-OP method by normalizing the DTT reduction rate according to the 9,10-phenanthrenequinone concentration, then evaluating the DTT reduction rates of the $PM_{2.5}$ samples. The experiment was conducted by injecting 0.2 mM DTT, 2.41 mM 5,5-dithio-bis (2-nitrobenzoic acid) (DTNB), and 500 mM potassium phosphate monobasic into the solution extracted from $PM_{2.5}$, followed by pH correction to 7.4 using 100 mM potassium phosphate dibasic. The mixture was then stirred at 37°C, and TNB was measured at an absorbance of 412 nm for a total of 4 times up to 40 min of the reaction using a multiflo FX (Multi-Mode Dispenser, Agilent Technologies, USA). The analysis was repeated for every 15 samples, and quinone samples were injected to maintain analysis accuracy and precision within 5%. The QDTT-OP results of this study, wherein the DTT reduction rate was normalized according to the 9,10-phenanthrenequinone concentration, are presented in Fig. S1.

3 Results

3.1 Result of Air Pollutant Measurements

The characteristics of the study area during the study period are presented in Table 1; Fig. 2. As shown in Fig. 2, the wind speed at the monitoring station was confirmed to be north-northeast at an average of 2.43 m/sec, indicating the influence of the adjacent roadway. The average temperature and humidity during the study period were found to be 23.4 °C and 60.27 RH%, respectively. The temperature and wind speed were seen to increase during the daytime hours from 09:00 to 20:00, while humidity decreased during the same period. The traffic flow around the monitoring site was found to be approximately 2,000 vehicles per hour on average, with approximately 3,000 vehicles per hour between 09:00 and 21:00, and approximately 500 vehicles per hour at 03:00 in the early morning. The speed of the vehicles was inversely proportional to the traffic flow, with

Table 1 Results of major compounds of gaseous and $PM_{2.5}$ compounds during the study

	Compounds	Unit	Average	Standard deviation
GAS	O_3	ppb	34.21	13.33
	CO	ppb	278	79
	CO_2	ppm	506	149
	SO_2	ppb	0.38	0.26
	NH_3	ppb	10.27	2.73
	NO	ppb	13.32	9.27
	NO_2	ppb	23.89	10.47
PM	$PM_{2.5}$	$\mu g/m^3$	12.04	6.07
	QDTT-OP	$\mu M/m^3$	0.24	0.06
	QDDT-OP/$PM_{2.5}$	$\mu M/\mu g$	0.03	0.05
	OC	$\mu g/m^3$	5.60	1.99
	WSOC	$\mu g/m^3$	3.72	1.31
	EC	$\mu g/m^3$	0.40	0.17
	eBC	$\mu g/m^3$	0.77	0.38
	NO_3^-	$\mu g/m^3$	1.08	0.93
	SO_4^{2-}	$\mu g/m^3$	1.89	1.08
	NH_4^+	$\mu g/m^3$	1.06	0.62
	Levoglucosan	$\mu g/m^3$	0.025	0.018
	1,2-BCA [1]	$\mu g/m^3$	0.011	0.007
	1,4-BCA [2]	$\mu g/m^3$	0.013	0.006
	MSA [3]	$\mu g/m^3$	0.026	0.018
	Al	$\mu g/m^3$	0.12	0.05
	Si	$\mu g/m^3$	0.30	0.19
	As	$\mu g/m^3$	0.01	0.02
	Pb	$\mu g/m^3$	0.02	0.02

[1] 1,2-benzene carboxylic acid

[2] 1,4-benzene carboxylic acid

[3] methyl sulfonic acid

speeds of 20–40 km/hr during the high traffic flow period from 09:00 to 21:00, and speeds of 45–60 km/hr between 21:00 and 06:00.

The observations for the average concentrations of gas pollutants were as follows (as presented in Table 1): O_3 34.21 ppb, CO 278 ppb, CO_2 506 ppb, NH_3 10.27 ppb, NO 13.32 ppb, and NO_2 23.89 ppb. Examining the changes in gas pollutants over time, O_3 showed a minimum value at 09:00 and then increased to a maximum value at 15:00, during the peak hours of photochemical reactions, before decreasing. The concentration of NO increased during the hours of increased traffic flow from 06:00 to 09:00 and then decreased after 12:00, during the peak hours of photochemical reactions. Meanwhile, NO_2 showed a similar increase during the hours of increased traffic flow from 06:00 to 09:00, but it continued to increase during the peak hours of photochemical reactions. This is interpreted as a result of the photochemical reaction of NO.

During the study period, the average concentration of $PM_{2.5}$ was 12.04 $\mu g/m^3$, with carbon components, ionic components, elemental component, and other components comprising 49.87%, 33.44%, 3.72%, and 12.96% of the analyzed constituents, respectively. In further detail, 93.25% of the carbon fraction was composed of OC whereas 6.75% was composed of EC. Using the OC/EC ratio-based EC tracer method, the OC/EC ratio of this study was determined to be 13.8, thus indicating a significant contribution of secondary organic carbon (SOC) in the carbon fraction (Bhowmik et al. 2021; Turpin and Huntzicker 1995). To identify the sources of SOC in the study area, the WSOC/OC ratio, temporal variations in OC, and particle number concentration were examined. Previous studies have determined that a WSOC/OC ratio of 0.1 indicates vehicular traffic, a value of 0.7 indicates biomass combustion, and a value of 0.9 indicates oxidized organic aerosols, which are primarily formed during daytime due to the influence of O_3, peroxy radicals, and VOCs generated by photolytic reactions (Daellenbach et al. 2016; Ram et al. 2012; Saarikoski et al. 2008; Weber et al. 2007). In this study, the average WSOC/OC ratio ranged from 0.36 to 0.95 with a mean value of 0.66 (Fig. S2). The WSOC/OC ratios were found to be 0.63 during daytime (09:00–18:00) and 0.78 during nighttime (18:00–09:00). Moreover, the particle number concentration increased during the photochemical reaction period, as shown in Fig. 2. Based on these results, it can be inferred that SOC is the primary carbonaceous material in the study area and that it is influenced by various emission sources, as observed in Fig. S1. Specifically, the daytime WSOC/OC ratio of 0.63 is likely attributable to the influence of vehicular traffic, whereas the nighttime WSOC/OC ratio of 0.78 is likely attributable to biomass combustion, which occurs in a relatively low-traffic environment where photochemical reactions are unlikely to occur.

The average concentrations of soluble ions contained in $PM_{2.5}$ were found to be 1.89 $\mu g/m^3$ for SO_4^{2-}, 1.08 $\mu g/m^3$ for NO_3^-, and 1.06 $\mu g/m^3$ for NH_4^+. Typically, SO_4^{2-}, NO_3^-, and NH_4^+ (SNA) account for the largest proportion of soluble ions in $PM_{2.5}$, and they are all known to be important factors in understanding the formation process of secondary inorganic aerosols (SIA) (Jimenez et al. 2009). The formation process of SIA by SNA involves the neutralization of acidic substances generated from SOx and NOx by the alkaline gas NH_3 present in the atmosphere, thus resulting in the formation of SIA substances (Hu et al. 2014; Pathak et al. 2004). Therefore, NH_3 is a key substance in the formation of SIA by SNA, and the mole concentrations of NH_4^+ and SO_4^{2-} in $PM_{2.5}$ are compared to evaluate the formation conditions of SIA formed by NH_3: If [NH_4^+]/[SO_4^{2-}] is greater than 1.5, the study area is evaluated as being ammonium-rich and an environment that facilitates SIA formation by SNA. Further, the neutralization reaction of NH_3 in the atmosphere primarily reacts first with the byproducts of
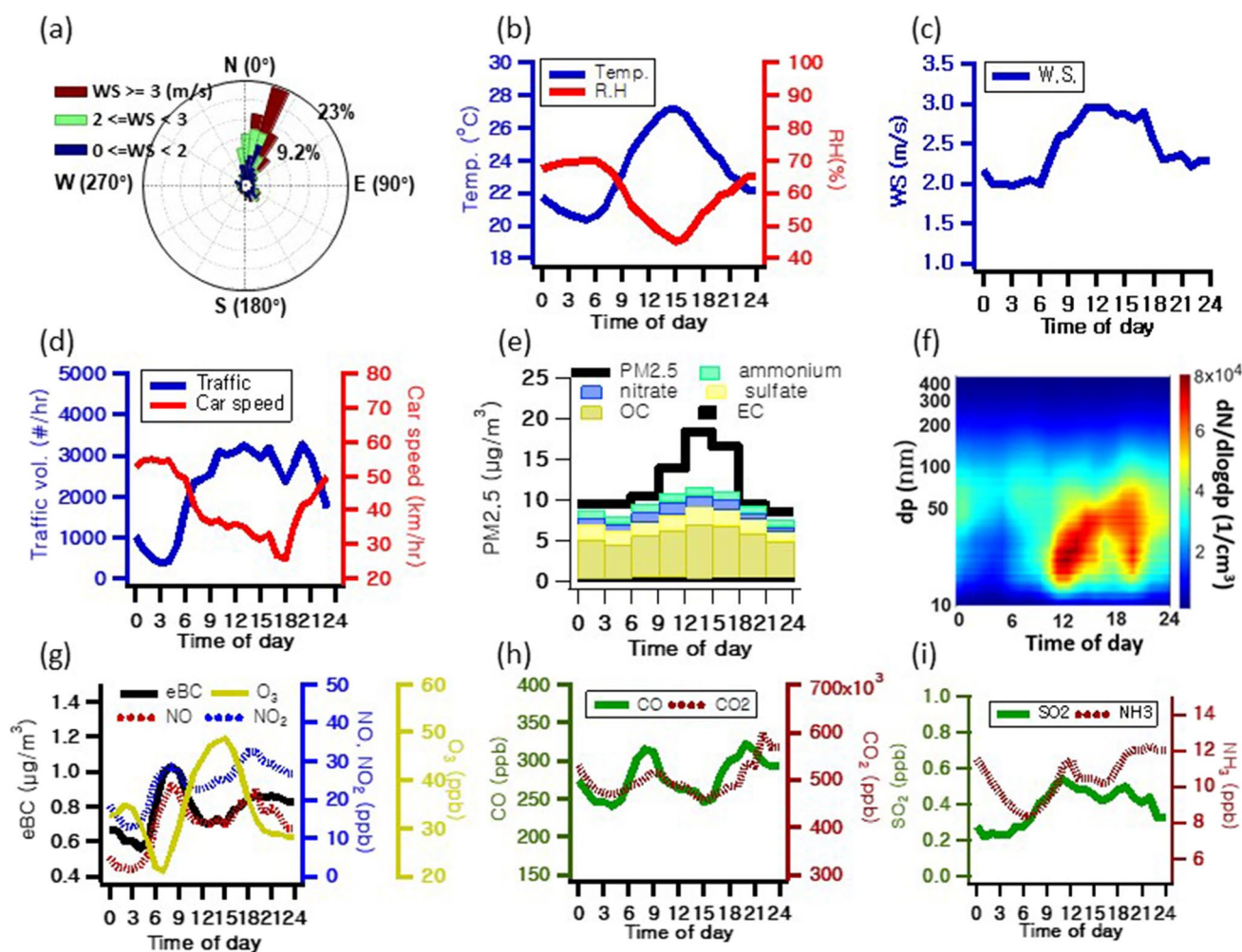
Fig. 2 a Wind rose, diurnal patterns of b temperature & relative humidity, c wind speed, d traffic volume & car speed, e PM$_{2.5}$ with major compounds, f size distributions, g eBC & major gaseous compounds, h CO & CO$_2$, and i SO$_2$ & NH$_3$

SOx and then with those of NOx. Therefore, as the mole ratio of [NO$_3^-$]/[SO$_4^{2-}$] in PM$_{2.5}$ increases, the contribution of NO$_3^-$ to SIA increases as well (Xu et al. 2019; Zhang et al. 2018). As shown in Fig. S3, [NH$_4^+$]/[SO$_4^{2-}$] in the study area was 1.5 or higher throughout the study period with an average value of 3.0, thus indicating that the study area was evaluated as being ammonium-rich and an environment that facilitated SIA formation by SNA. [NO$_3^-$]/[SO$_4^{2-}$] was found to be relatively high, at 0.88 on average, thus indicating that SO$_4^{2-}$ contributes significantly to SIA formation in the study area. Moreover, as shown in Fig. S3, the correlation between [NH$_4^+$]/[SO$_4^{2-}$] and [NO$_3^-$]/[SO$_4^{2-}$] is moderately high at r^2 0.7. Considering that the study area is in an ammonium-rich state, NO$_3^-$ is estimated to be the component that triggers high concentrations of SIA in the study area. Further, given that SIA components account for 33.44% of PM$_{2.5}$ in the study area, NO$_3^-$ is expected to have a significant impact on PM$_{2.5}$ concentrations.

3.2 Atmospheric Pollutant Emission Sources

To estimate the emission sources of air pollutants in the study area, a PMF model and flux analysis—which measures concentration times wind speed based on measurement stations—were performed. The PMF model is a receptor model that is used to estimate the contribution of major pollution sources in the study area by analyzing the potential source factors based on the data measured at the receptor sites (Lu et al. 2018). The PMF model uses factor analysis to extract common factors by extracting the interrelationships of various variables into a small number of factors, thereby identifying the degree of influence received by each variable and characteristics of the group (Cesari et al. 2016; Watson et al. 2008). The PMF input data are the items observed in the study area, and the result on the source classification table calculated using PMF is six, as shown in Fig. 3, which includes vehicle emission, resuspended dust, biomass
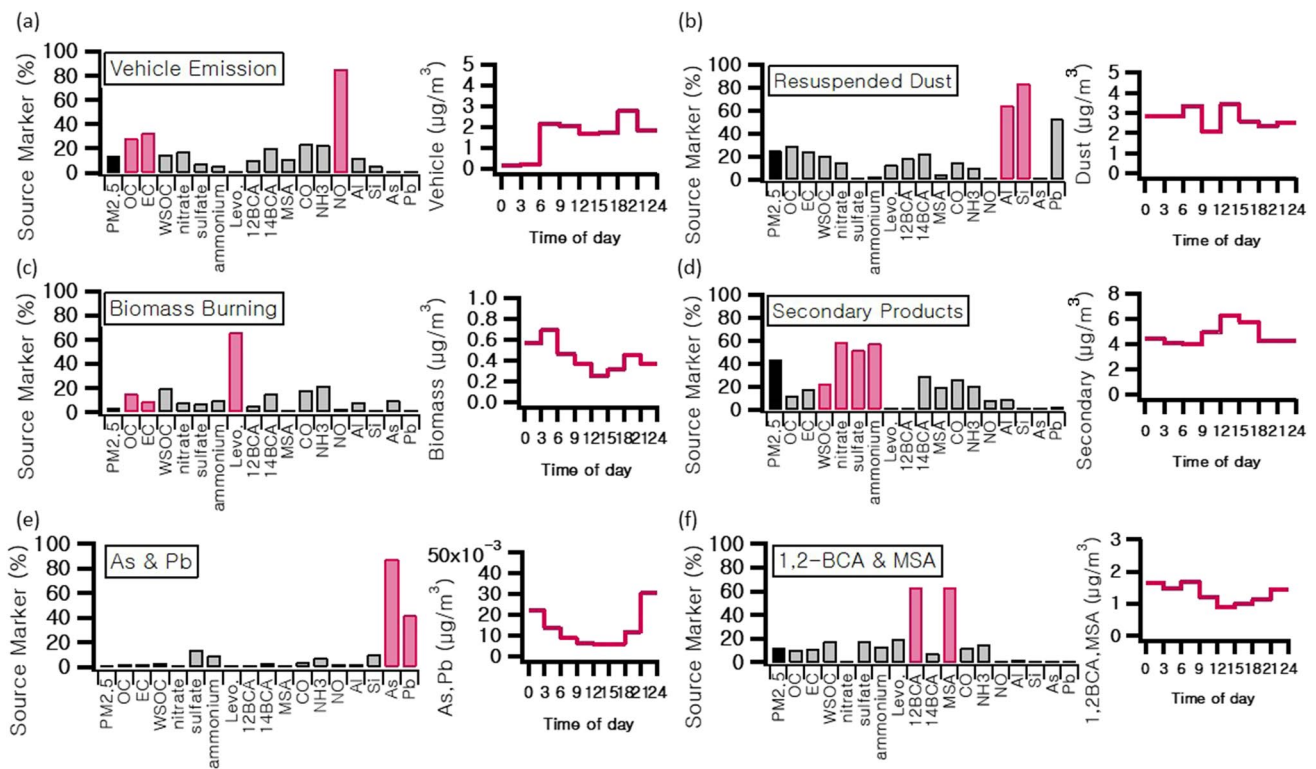
Fig. 3 Source profiles and diurnal patterns of results from **a** Vehicle Emission, **b** Resuspended Dust, **c** Biomass Burning, **d** Secondary Products, **e** As & Pb, and **f** 1,2-BCA & MSA sources of Positive Matrix Factorization (PMF)

burning, secondary product, 1,2-BCA & MSA, and As & Pb. The criteria for the cause classification table were selected by referring to the time-based emission characteristics criteria and major emission material data presented in previous studies, as shown in Fig. 3.

The compounds used for vehicle emission are the vehicle exhaust substances—such as OC, EC, and NO—that increased similarly to the increase in traffic around the measurement station (Bhowmik et al. 2021; Hueglin et al. 2006; Wild et al. 2017). Resuspended dust is mainly composed of Al and Si found in surface materials, and it is expected to represent non-exhaust particles around the measurement station. However, there may be limitations in distinguishing the emission sources of resuspended dust, as non-exhaust particles can be affected by various environmental factors, such as population and traffic flow as well as external inflow. Moreover, the measurement station was located about 10 m away from the road and was situated in a park, at which there were various events during the study period, thus resulting in a relatively high level of population movement. Therefore, it is difficult to interpret the emission sources of resuspended dust in detail, and only the impact of non-exhaust particles on $PM_{2.5}$ can be evaluated accurately.

Biomass burning exhibits high concentrations, mainly during nighttime, and it was characterized using emissions of OC, EC, and organic tracer compounds such as levoglucosan, which can only be generated by the breakdown of cellulose and hemicellulose at temperatures exceeding 300℃ (Achad et al. 2018; Simoneit 1999). Therefore, levoglucosan is used as an indicator of $PM_{2.5}$ from biomass burning. The secondary products targeted were WSOC and SNA, which are precursors to the formation of SOC and SIA, and which showed increasing trends during photochemical reaction times. As and Pb were identified as components that primarily increase during nighttime, thus exhibiting different emission characteristics compared to the other analyzed substances. The sources of As and Pb include industrial settings and transportation, combustion of fossil fuels and tires, and resuspended dust (Charron et al. 2019; Suvarapu and Baek 2017). Considering the location of the monitoring station, i.e., in the city center, the increase in As and Pb during nighttime, and the faster vehicular speed at night, the findings regarding As and Pb in this study could be interpreted as the result of heating activities such as tire wear or fossil fuel combustion.

1,2-BCA and MSA are used as source apportionment tracers for the long-range transport of $PM_{2.5}$ through the ocean to the western side of the monitoring site, where MSA is a marker for marine influence and 1,2-BCA is a widely used molecular marker for various atmospheric chemical

processes (Bae et al. 2006; Yu et al. 2019). Therefore, 1,2-BCA and MSA are source apportionment components that are used to evaluate the emission sources of $PM_{2.5}$ transported over long distances through the ocean to the monitoring site.

The contributions of atmospheric pollutants by source category in the study area were obtained using the PMF model and presented in Table 2. As can be seen in the table, secondary products were found to have the greatest impact on $PM_{2.5}$ in the study area, accounting for 43.7% of the total contributions, followed by resuspended dust (25.4%), vehicle emissions (14.4%), 1,2-BCA & MSA (12.3%), biomass burning (4.1%), and As & Pb (0.1%). When comparing with previous studies on PMF source contributions, measurements obtained from a park in the same urban area (Seoul) exhibited similarities to the findings of this study in terms of vehicle emissions (14.4%) and total contributions (43.2%), while biomass burning (13.8%) showed variations (Song

et al. 2022). Among urban areas outside the Seoul region, Jakarta, Indonesia (dry season), revealed total contributions (25%), vehicle emissions (22%), and biomass burning (16%). In contrast, Florence, Italy, demonstrated total contributions (42%), vehicle emissions (20%), and biomass burning (20%). These variations in PMF source contributions were observed based on urban area characteristics (Lestari and Mauliadi 2009; Nava et al. 2020). The PMF analysis revealed that the study area is significantly affected by secondary organic carbon (SOC) and secondary inorganic aerosol (SIA) products. However, as was explained in the previous section, resuspended dust is partially caused by vehicle exhaust emissions, which suggests that vehicle traffic could have a greater impact on the atmospheric environment than the PMF model classifies as vehicle emissions. Therefore, to more accurately estimate the specific sources of atmospheric pollution in the study area, the relationship between vehicle traffic volume and air pollutant concentrations was examined using flux analysis.

3.3 Relationship with Flux and Traffic Volume

The target compounds for flux analysis included $PM_{2.5}$ mass, OC including SOC concentration, Al and Si from the resuspended dust category of PMF source apportionment, NO as a precursor of secondary inorganic aerosols, and eBC and CO as vehicle exhaust pollutants that can represent traffic-related emissions. The results of the flux analysis are shown in Fig. 4, where it can be seen that there are high correlations between traffic volume and $PM_{2.5}$, OC, Al, eBC, CO, and NO. However, these correlations were only observed when

Table 2 Results of Positive Matrix Factorization (PMF) during the study

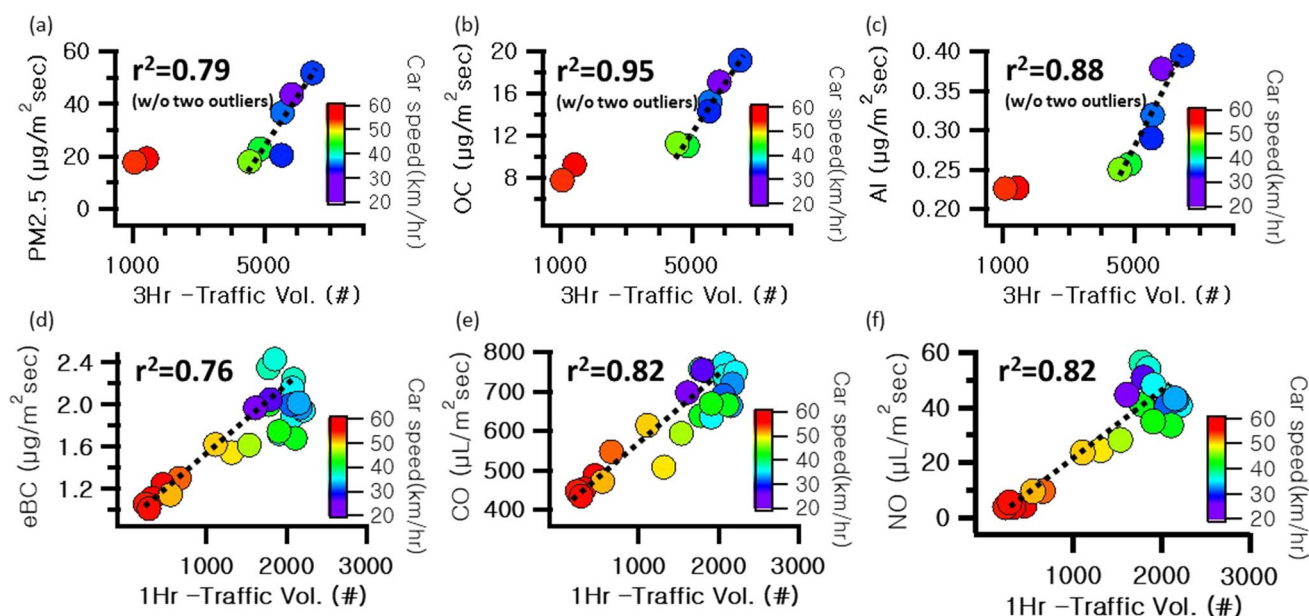| Type of Source	Concentration ($\mu g/m^3$)	Relative Ratio (%)
Vehicle emission	1.56	14.4
Resuspended dust	2.76	25.4
Biomass burning	0.45	4.1
Secondary product	4.75	43.7
1,2-BCA & MSA	1.33	12.3
As & Pb	0.01	0.1

Fig. 4 Relations between flux and traffic volume

the vehicle speed was below 50 km/hr for PM$_{2.5}$, OC, and Al, while there was no correlation when the speed exceeded 50 km/hr. The disparity in correlation between vehicle flow and vehicle emissions based on speeds exceeding and below 50 km/hr is presumed to result from variations in fuel consumption linked to vehicular travel speed. Generally, when vehicle travel speed increases from 40 km/hr to 80 km/hr, the rate of fuel combustion consumption rises by approximately 94%. As this fuel combustion consumption escalates, emissions from vehicular combustion of fossil fuels also increase (Song et al. 2023; Wang et al. 2008). Therefore, the vehicle speeds of 50 km/hr and above presented in our study results are deemed reflective of the increment in fuel combustion consumption. Nevertheless, it can be clearly confirmed from the flux analysis that air pollutants in the study area are affected by traffic volume, and most importantly, that the correlation of flux allows for the estimation of the reduction in air pollutant emissions due to the decrease in traffic volume. Thus, based on the regression equation derived from the correlation between air pollutants and vehicular traffic flow rate presented in Fig. 4, the reduction in vehicular traffic can provide an estimate of the reduction in air pollutants. However, as indicated by the results of PMF analysis, the study area is subject to various emission sources outside of vehicular traffic, including 1,2-BCA & MSA and biomass combustion. Therefore, the reduction in major components of PM$_{2.5}$, such as SOC and SIA, cannot be solely attributed to the results obtained from flux analysis. Nonetheless, our findings clearly indicate a close relationship between air pollution in densely populated urban areas, such as the study area, and vehicular traffic flow rate, thereby suggesting the potential to derive methods to reduce urban air pollution in the future based on these results.

3.4 Relationship with Biomass Burning Source and Oxidative Potential

The monitoring station was installed in Gwanghwamun Square, as shown in Fig. 1. To analyze the sources of human health-hazardous emissions in the PM$_{2.5}$ in the study area, QDTT-OP analysis was performed, and the average concentration of QDTT-OP was found to be 0.24 μM/m^3. In examining the correlation between PM$_{2.5}$ concentration and QDTT-OP, as shown in Fig. 5a, no correlation was found between PM$_{2.5}$ concentration and DTT-OP. Previous studies have reported that DTT-OP is induced by metal components or SOA in PM$_{2.5}$ (Bates et al. 2019; Shiraiwa et al. 2017). However, these previous studies have shown conflicting results, and it is still difficult to clearly identify the components in PM$_{2.5}$ that cause an increase in DTT-OP. Further, since an increase in DTT-OP can be due to various factors such as particle size, emission form of PM, and various components in PM, it is not easy to determine the characteristics of PM that actually increase DTT-OP. Therefore, rather than determining the characteristics of PM that increase DTT-OP, the present work evaluated QDTT-OP based on emission sources. This study evaluated human health-hazardous emissions sources based on the six source categories of vehicle emission, resuspended dust, biomass burning, secondary product, 1,2-BCA & MSA, As & Pb, which were used in the PMF analysis.

As a result, it was found that QDTT-OP was induced by biomass burning, which was consistent with the time series of biomass burning in the six causative classification tables, as shown in Fig. 5a, b. Although QDTT-OP did not correlate with the concentration of PM$_{2.5}$ and the time series of the other five causative classification tables, when the

Fig. 5 Relations between QDTT-OP and PM$_{2.5}$ mass and biomass burning source
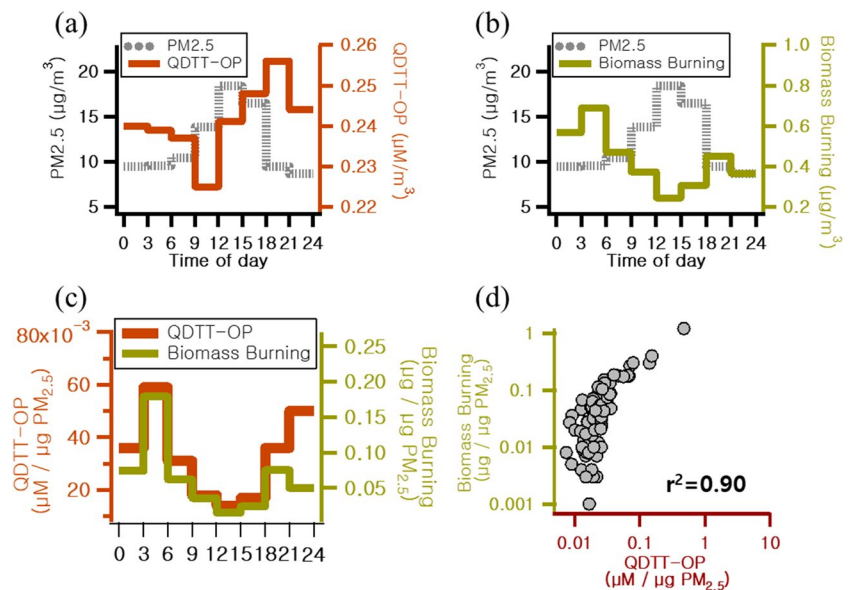
biomass burning of the causative classification tables was converted to PM$_{2.5}$ mass, the time series of QDTT-OP and biomass burning showed a high correlation, as can be seen in Fig. 5c. Specifically, Fig. 5d shows that there was a very high correlation between QDTT-OP/PM$_{2.5}$ μM/μg and biomass burning/PM$_{2.5}$ μg/μg. These results signify two crucial aspects. First, the emission source affecting the human health toxicity of PM$_{2.5}$ in the study area is biomass burning. This aligns with previous research findings, indicating the health toxicity of PM$_{2.5}$ originating from biomass burning (Daellenbach et al. 2020). Second, it highlights that the human health toxicity of PM$_{2.5}$ is predominantly governed by emission sources, surpassing particle concentration and compositional characteristics. This underscores a significant revelation: mitigating the human health toxicity of PM$_{2.5}$ necessitates foremost management of emission sources with higher toxicity. To date, efforts to reduce the human health toxicity of PM$_{2.5}$ have largely focused on diminishing PM$_{2.5}$ concentrations. This has involved identifying the primary constituents and generation mechanisms of PM$_{2.5}$, driving efforts towards reducing its absolute quantity. Undoubtedly, these endeavors are anticipated to contribute to decreasing the human health toxicity of PM$_{2.5}$.

However, as evidenced by the findings in this study, the human health toxicity of PM$_{2.5}$ is greatly influenced by emission sources, outweighing the effects of PM$_{2.5}$ concentration and composition. From these outcomes, it is evident that even at lower PM$_{2.5}$ concentrations, the human health toxicity can be elevated based on emission sources. Consequently, to mitigate the human health toxicity of PM$_{2.5}$, a shift is required from merely managing existing PM$_{2.5}$ concentrations towards targeting emission sources with higher toxicity. This necessitates a prior assessment of emission-specific human health toxicity associated with PM$_{2.5}$ and, based on such assessments, a more economically and efficiently oriented PM$_{2.5}$ management strategy can be envisaged.

4 Conclusion

In this study, we assessed the air quality in densely populated urban areas and investigated the emission sources that affect urban air quality and contribute to the human health risks associated with urban PM based on the obtained results. The study revealed that urban air quality is significantly influenced by the emissions from secondary pollutants and vehicle traffic. Moreover, flux analysis demonstrated that reducing urban vehicle emissions directly improves air quality. Further, an analysis of the factors affecting human health risks associated with emission sources indicated that biomass burning emissions have a major impact. This study provides indicators for reducing vehicle emissions to improve urban air quality and emission sources that need to

be controlled to reduce human health risks. The results of this study are expected to serve as fundamental data for managing urban PM and reducing the associated human health risks, which are global concerns.

Declarations

Conflict of Interest The authors declare that they have no conflicts of interest.

References

Achad, M., Caumo, S., de Castro Vasconcellos, P., Bajano, H., Gómez, D., Smichowski, P.: Chemical markers of biomass burning: Determination of levoglucosan, and potassium in size-classified atmospheric aerosols collected in Buenos Aires, Argentina by different analytical techniques. Microchem. J. **139**, 181–187 (2018). https://doi.org/10.1016/j.microc.2018.02.016

Auerbach, A., Hernandez, M.L.: The effect of environmental oxidative stress on airway inflammation. Curr. Opin. Allergy Clin. Immunol. **12**(2), 133 (2012)

Bae, M.-S., Schauer, J.J., Turner, J.R.: Estimation of the monthly average ratios of organic mass to organic carbon for fine particulate matter at an urban site. Aerosol Sci. Technol. **40**(12), 1123–1139 (2006)

Bates, J.T., Fang, T., Verma, V., Zeng, L., Weber, R.J., Tolbert, P.E., Russell, A.G.: Review of Acellular assays of ambient particulate matter oxidative potential: Methods and relationships with composition, sources, and health effects. Environ. Sci. Technol. **53**(8), 4003–4019 (2019). https://doi.org/10.1021/acs.est.8b03430

Berhane, K., Zhang, Y., Linn, W.S., Rappaport, E.B., Bastain, T.M., Salam, M.T., Gilliland, F.D.: The effect of ambient air pollution on exhaled nitric oxide in the Children's Health Study. Eur. Respir. J. **37**(5), 1029 (2011). https://doi.org/10.1183/09031936.00081410

Bhowmik, H.S., Naresh, S., Bhattu, D., Rastogi, N., Prévôt, A.S.H., Tripathi, S.N.: Temporal and spatial variability of carbonaceous species (EC; OC; WSOC and SOA) in PM2.5 aerosol over five sites of Indo-Gangetic Plain. Atmos. Pollut. Res. **12**(1), 375–390 (2021). https://doi.org/10.1016/j.apr.2020.09.019

Brown, M.S., Sarnat, S.E., DeMuth, K.A., Brown, L.A.S., Whitlock, D.R., Brown, S.W., Fitzpatrick, A.M.: Residential proximity to

a major roadway is associated with features of asthma control in children. PLoS ONE **7**(5), e37044 (2012)

Cesari, D., Donateo, A., Conte, M., Contini, D.: Inter-comparison of source apportionment of PM10 using PMF and CMB in three sites nearby an industrial area in central Italy. Atmos. Res. **182**, 282–293 (2016). https://doi.org/10.1016/j.atmosres.2016.08.003

Charron, A., Polo-Rehn, L., Besombes, J.L., Golly, B., Buisson, C., Chanut, H., Jaffrezo, J.L.: Identification and quantification of particulate tracers of exhaust and non-exhaust vehicle emissions. Atmos. Chem. Phys. **19**(7), 5187–5207 (2019). https://doi.org/10.5194/acp-19-5187-2019

Choe, S., Oh, S.-H., Song, M., Kim, E., Lee, Y., Seo, S., Park, G., Kim, M., Lee, T., Nae, M.-S.: Seasonal oxidation potential of vehicle emission using tunnel flow coefficient. J. Korean Soc. Atmos. Environ. **38**(2), 294–303 (2022). https://doi.org/10.5572/KOSAE.2022.38.2.294. (in Korea Abstract)

Cohen, A.J., Brauer, M., Burnett, R., Anderson, H.R., Frostad, J., Estep, K., Forouzanfar, M.H.: Estimates and 25-year trends of the global burden of disease attributable to ambient air pollution: An analysis of data from the Global Burden of Diseases Study 2015. The Lancet **389**(10082), 1907–1918 (2017). https://doi.org/10.1016/S0140-6736(17)30505-6

Daellenbach, K.R., Bozzetti, C., Křepelová, A., Canonaco, F., Wolf, R., Zotter, P., Prévôt, A.S.H.: Characterization and source apportionment of organic aerosol using offline aerosol mass spectrometry. Atmos. Meas. Tech. **9**(1), 23–39 (2016). https://doi.org/10.5194/amt-9-23-2016

Daellenbach, K.R., Uzu, G., Jiang, J., Cassagnes, L.-E., Leni, Z., Vlachou, A., Stefenelli, G., Canonaco, F., Weber, S., Segers, A., Kuenen, J.J.P., Schaap, M., Favez, O., Albinet, A., Aksoyoglu, S., Dommen, J., Baltensperger, U., Geiser, M., El Haddad, I., Jaffrezo, J.-L., Prévôt, A.S.H.: Sources of particulate-matter air pollution and its oxidative potential in Europe. Nature **587**(7834), 414–419 (2020). https://doi.org/10.1038/s41586-020-2902-8

Delfino, R.J., Staimer, N., Vaziri, N.D.: Air pollution and circulating biomarkers of oxidative stress. Air Qual. Atmos. Health **4**(1), 37–52 (2011). https://doi.org/10.1007/s11869-010-0095-2

Dominici, F., Peng, R.D., Bell, M.L., Pham, L., McDermott, A., Zeger, S.L., Samet, J.M.: Fine particulate air pollution and hospital admission for cardiovascular and respiratory diseases. JAMA **295**(10), 1127–1134 (2006)

Esposito, S., Tenconi, R., Lelii, M., Preti, V., Nazzari, E., Consolo, S., Patria, M.F.: Possible molecular mechanisms linking air pollution and asthma in children. BMC Pulm. Med. **14**(1), 31 (2014). https://doi.org/10.1186/1471-2466-14-31

Fann, N., Lamson, A.D., Anenberg, S.C., Wesson, K., Risley, D., Hubbell, B.J.: Estimating the National Public Health Burden Associated with exposure to ambient PM2.5 and ozone. Risk Anal. **32**(1), 81–95 (2012). https://doi.org/10.1111/j.1539-6924.2011.01630.x

Forouzanfar, M.H., Afshin, A., Alexander, L.T., Anderson, H.R., Bhutta, Z.A., Biryukov, S., Murray, C.J.L.: Global, regional, and national comparative risk assessment of 79 behavioural, environmental and occupational, and metabolic risks or clusters of risks, 1990–2015: A systematic analysis for the global burden of Disease Study 2015. The Lancet **388**(10053), 1659–1724 (2016). https://doi.org/10.1016/S0140-6736(16)31679-8

Gao, D., Mulholland, J.A., Russell, A.G., Weber, R.J.: Characterization of water-insoluble oxidative potential of PM2.5 using the dithiothreitol assay. Atmos. Environ. **224**, 117327 (2020). https://doi.org/10.1016/j.atmosenv.2020.117327

Hu, G., Zhang, Y., Sun, J., Zhang, L., Shen, X., Lin, W., Yang, Y.: Variability, formation and acidity of water-soluble ions in PM2.5 in Beijing based on the semi-continuous observations. Atmos. Res. **145–146**, 1 (2014). https://doi.org/10.1016/j.atmosres.2014.03.014

Hueglin, C., Buchmann, B., Weber, R.O.: Long-term observation of real-world road traffic emission factors on a motorway in Switzerland. Atmos. Environ. **40**(20), 3696–3709 (2006). https://doi.org/10.1016/j.atmosenv.2006.03.020

IARC: IARC Monographs on the Evaluation of Carcinogenic Risks to Humans. Agents Classified by the IARC Monographs, vol. 112. Retrieved January 22, 2021 (2017)

IARC: Some non-heterocyclic polycyclic aromatic hydrocarbons and some related exposures. In: IARC Monographs on the Evaluation of Carcinogenic Risks to Humans, vol. 92. International Agency for Research on Cancer, Lyon (2010)

Im, U., Brandt, J., Geels, C., Hansen, K.M., Christensen, J.H., Andersen, M.S., Galmarini, S.: Assessment and economic valuation of air pollution impacts on human health over Europe and the United States as calculated by a multi-model ensemble in the framework of AQMEII3. Atmos. Chem. Phys. **18**(8), 5967–5989 (2018). https://doi.org/10.5194/acp-18-5967-2018

Jimenez, J.L., Canagaratna, M., Donahue, N., Prevot, A., Zhang, Q., Kroll, J.H., Ng, N.: Evolution of organic aerosols in the atmosphere. Science **326**(5959), 1525–1529 (2009). https://doi.org/10.1126/science.1180353

Katsouyanni, K., Touloumi, G., Samoli, E., Gryparis, A., Le Tertre, A., Monopolis, Y., Schwartz, J.: Confounding and Effect Modification in the Short-Term Effects of Ambient Particles on Total Mortality: Results from 29 European Cities within the APHEA2 Project. Epidemiology **12**(5), 521–531. Retrieved from (2001). http://www.jstor.org/stable/3703877

Kelly, F.J., Fussell, J.C.: Size, source and chemical composition as determinants of toxicity attributable to ambient particulate matter. Atmos. Environ. **60**, 504–526 (2012). https://doi.org/10.1016/j.atmosenv.2012.06.039

Lestari, P., Mauliadi, Y.D.: Source apportionment of particulate matter at urban mixed site in Indonesia using PMF. Atmos. Environ. **43**(10), 1760–1770 (2009). https://doi.org/10.1016/j.atmosenv.2008.12.044

Li, Q., Wyatt, A., Kamens, R.M.: Oxidant generation and toxicity enhancement of aged-diesel exhaust. Atmos. Environ. **43**(5), 1037–1042 (2009). https://doi.org/10.1016/j.atmosenv.2008.11.018

Lin, M., Yu, J.Z.: Dithiothreitol (DTT) concentration effect and its implications on the applicability of DTT assay to evaluate the oxidative potential of atmospheric aerosol samples. Environ. Pollut. **251**, 938–944 (2019). https://doi.org/10.1016/j.envpol.2019.05.074

Lodovici, M., Bigagli, E.: Oxidative stress and air pollution exposure. J. Toxicol. (2011). https://doi.org/10.1155/2011/487074

Lu, Z., Liu, Q., Xiong, Y., Huang, F., Zhou, J., Schauer, J.J.: A hybrid source apportionment strategy using positive matrix factorization (PMF) and molecular marker chemical mass balance (MM-CMB) models. Environ. Pollut. **238**, 39–51 (2018). https://doi.org/10.1016/j.envpol.2018.02.091

Matsumoto, R., Umezawa, N., Karaushi, M., Yonemochi, S.-I., Sakamoto, K.: Comparison of ammonium deposition flux at Roadside and at an agricultural area for long-term monitoring: Emission of Ammonia from Vehicles. Water Air Soil Pollut. **173**(1), 355–371 (2006). https://doi.org/10.1007/s11270-006-9088-z

Nava, S., Calzolai, G., Chiari, M., Giannoni, M., Giardi, F., Becagli, S., Severi, M., Traversi, R., Lucarelli, F.: Source apportionment of PM2.5 in Florence (Italy) by PMF analysis of aerosol composition records. Atmosphere **11**, 484 (2020). https://doi.org/10.3390/atmos11050484

Patel, M.M., Chillrud, S.N., Deepti, K.C., Ross, J.M., Kinney, P.L.: Traffic-related air pollutants and exhaled markers of airway inflammation and oxidative stress in New York City adolescents. Environ. Res. **121**, 71–78 (2013). https://doi.org/10.1016/j.envres.2012.10.012

Pathak, R.K., Yao, X., Chan, C.K.: Sampling artifacts of acidity and ionic species in PM2. 5. Environ. Sci. Technol. **38**(1), 254–259 (2004). https://doi.org/10.1021/es0342244

Perrino, C., Catrambone, M., Di Menno, A., Allegrini, I.: Gaseous ammonia in the urban area of Rome, Italy and its relationship with traffic emissions. Atmos. Environ. **36**(34), 5385–5394 (2002). https://doi.org/10.1016/S1352-2310(02)00469-7

Ram, K., Sarin, M., Sudheer, A., Rengarajan, R.: Carbonaceous and secondary inorganic aerosols during wintertime fog and haze over urban sites in the Indo-Gangetic Plain. Aerosol Air Qual. Res. **12**(3), 359–370 (2012)

Saarikoski, S., Timonen, H., Saarnio, K., Aurela, M., Järvi, L., Keronen, P., Hillamo, R.: Sources of organic carbon in fine particulate matter in northern european urban air. Atmos. Chem. Phys. **8**(20), 6281–6295 (2008). https://doi.org/10.5194/acp-8-6281-2008

Shiraiwa, M., Ueda, K., Pozzer, A., Lammel, G., Kampf, C.J., Fushimi, A., Sato, K.: Aerosol health effects from molecular to global scales. Environ. Sci. Technol. **51**(23), 13545–13567 (2017). https://doi.org/10.1021/acs.est.7b04417

Simoneit, B.R.T.: A review of biomarker compounds as source indicators and tracers for air pollution. Environ. Sci. Pollut. Res. **6**(3), 159–169 (1999). https://doi.org/10.1007/BF02987621

Song, M., Kim, E., Lee, Y., Oh, S.-H., Yu, G.-H., Choe, S., Park, G., Lee, T., Bae, M.-S.: Seasonal vehicle emission rate of chemical compounds related to fuel type from on-road tunnel measurement. Atmos. Environ. **305**, 119777 (2023). https://doi.org/10.1016/j.atmosenv.2023.119777

Song, M., Park, J., Lim, Y., Oh, S.-H., Lee, J.Y., Lee, K.-H., Ro, C.-U., Bae, M.-S.: Long-range transport impacts from biomass burning and secondary pollutant sources based on receptor models during KORUS-AQ campaign. Atmos. Environ. **276**, 119060 (2022). https://doi.org/10.1016/j.atmosenv.2022.119060

Suvarapu, L.N., Baek, S.-O.: Determination of heavy metals in the ambient atmosphere: A review. Toxicol. Ind. Health **33**(1), 79–96 (2017). https://doi.org/10.1177/0748233716654 8

Turpin, B.J., Huntzicker, J.J.: Identification of secondary organic aerosol episodes and quantitation of primary and secondary organic aerosol concentrations during SCAQS. Atmos. Environ. **29**(23), 3527–3544 (1995). https://doi.org/10.1016/1352-2310(94)00276-Q

Wang, H., Fu, L., Zhou, Y., Li, H.: Modelling of the fuel consumption for passenger cars regarding driving characteristics. Transp. Res. Part D: Transp. Environ. **13**(7), 479–482 (2008). https://doi.org/10.1016/j.trd.2008.09.002

Watson, J.G., Chen, A., Chow, L.W., Doraiswamy, J.C., Lowenthal, P.: Source apportionment: Findings from the U.S. Supersites Program. J Air Waste Manag Assoc **58**(2), 265–288 (2008). https://doi.org/10.3155/1047-3289.58.2.265

Weber, R.J., Sullivan, A.P., Peltier, R.E., Russell, A., Yan, B., Zheng, M., Edgerton, E.: A study of secondary organic aerosol formation in the anthropogenic-influenced southeastern United States. J. Geophys. Research: Atmos. **112**, D13 (2007). https://doi.org/10.1029/2007JD008408

Wild, R.J., Dubé, W.P., Aikin, K.C., Eilerman, S.J., Neuman, J.A., Peischl, J., Brown, S.S.: On-road measurements of vehicle NO2/NOx emission ratios in Denver, Colorado, USA. Atmos. Environ. **148**, 182–189 (2017). https://doi.org/10.1016/j.atmosenv.2016.10.039

Xu, W., Liu, X., Liu, L., Dore, A.J., Tang, A., Lu, L., Zhang, F.: Impact of emission controls on air quality in Beijing during APEC 2014: Implications from water-soluble ions and carbonaceous aerosol in PM2.5 and their precursors. Atmos. Environ. **210**, 241–252 (2019). https://doi.org/10.1016/j.atmosenv.2019.04.050

Yang, J., Shi, B., Shi, Y., Marvin, S., Zheng, Y., Xia, G.: Air pollution dispersal in high density urban areas: Research on the triadic relation of wind, air pollution, and urban form. Sustain. Cities Soc. **54**, 101941 (2020). https://doi.org/10.1016/j.scs.2019.101941

Yu, Q., Chen, J., Qin, W., Cheng, S., Zhang, Y., Ahmad, M., Ouyang, W.: Characteristics and secondary formation of water-soluble organic acids in PM1, PM2.5 and PM10 in Beijing during haze episodes. Sci. Total Environ. **669**, 175–184 (2019). https://doi.org/10.1016/j.scitotenv.2019.03.131

Zanobetti, A., Franklin, M., Koutrakis, P., Schwartz, J.: Fine particulate air pollution and its components in association with cause-specific emergency admissions. Environ. Health **8**(1), 58 (2009). https://doi.org/10.1186/1476-069X-8-58

Zhang, Y., Lang, J., Cheng, S., Li, S., Zhou, Y., Chen, D., Wang, H.: Chemical composition and sources of PM1 and PM2.5 in Beijing in autumn. Sci. Total Environ. **630**, 72–82 (2018). https://doi.org/10.1016/j.scitotenv.2018.02.151